The flapping of a flag. Numerical investigation of a Kelvin–Helmholtz type instability

Bailo BALDE Jocelyn ÉTIENNE

CNRS – Université J. Fourier Grenoble I, UMR 5588, Laboratoire Interdisciplinaire de Physique, F38402, Grenoble

Résumé

L'interaction d'une structure fine et inextensible avec un écoulement est connu pour donner lieu à une déstabilisation en-deça de la transition turbulente dans le fluide. Lorsque l'élasticité de courbure de la structure est faible, cette instabilité est de type Kelvin–Helmholtz. Elle est excitée par la différence d'inertie entre fluide et structure mais elle est stabilisée par la tension. Par simulation numérique aux éléments finis, utilisant une approche de multiplicateur de Lagrange pour la tension, nous décrivons la déstabilisation qui en résulte.

Abstract

An instability is known to arise from the interaction of a thin, inextensible structure with a flow well below transition to turbulence in the fluid. For a small bending rigidity of the structure, the instability is of Kelvin–Helmholtz type. It is excited by the momentum difference between fluid and structure, but is stabilised by the drag-generated tension in the structure. This instability is analysed using finite elements numerical simulations with a Lagrange multiplier approach for the tension.

1 Introduction

The flapping of a flag in the wind is a common day experience, but remains one of these simple problems that may elicit a controversy. Indeed, the notion of flag flapping may refer to several distinct regimes pertaining to different types of instabilities. We will only mention the different origins of these flapping regimes and related studies, a quite thorough review of recent literature on this subject may be found in [1].

One regime corresponds to the aerodynamic fluttering of a thin structure: this is encountered for structures with a large inertia (high surfacic mass compared to added mass from the surrounding fluid) and large bending rigidity [2]. When the fluid inertia is large and dominates, then vortices shed from the pole at which the flag is fixed can destabilise it [3]. However, below transition to turbulent flow, an instability of Kelvin–Helmholtz type can develop [1]: just as for mixing layers, it is promoted by a difference in momentum of two parts of the system, here, the fluid layer on both sides of the flag and the flag itself. The tension in the flag however, which is generated by the friction force that the fluid exerts on it, tends to stabilise it. This regime is found for low bending rigidity and finite inertia of both the structure and the fluid. This is the particular regime at which we will focus in this paper.

In order to study this regime numerically, it is of importance to use a highly stable numerical scheme with an accurate implementation of the inextensibility of the structure. However, the numerical algorithms used for fluid-structure interactions are generally coupled only through fixed-point or Newton-Raphson iterations [e.g. 4], and fully-coupled (monolithic) methods remain the exception [5]. Algorithms using a fixed-point coupling between structure and fluid dynamics are indeed prone to numerical unstability when the inertia of the structure is not dominant, as reported in [1], despite using conforming grids between the fluid and structure.

Here we employ a novel monolithic approach specialized for interactions between fluids and thin structures, introduced in [6]. This method allows to incorporate the thin structure equations as a boundary condition of the fluid problem. We demonstrate its capability to address the flag flapping problem in a range of parameters that had not been explored so far.

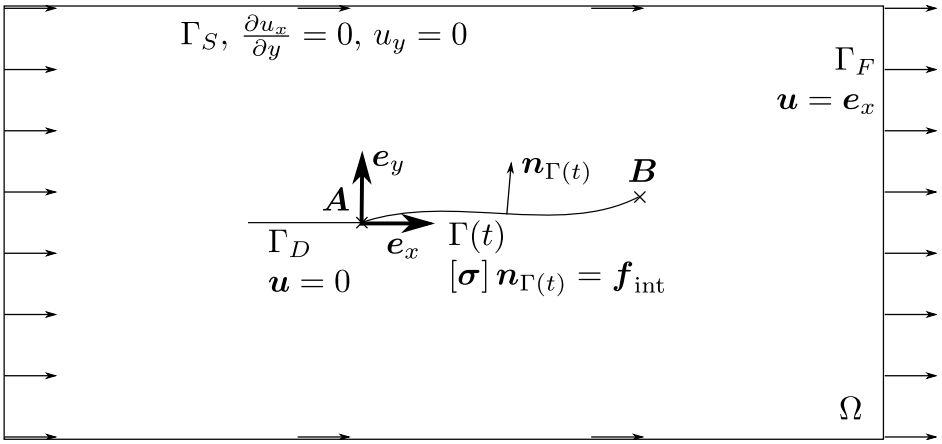

Figure 1: Geometry and boundary conditions for the flow past a flag problem. The flow past a plate can be simulated when the curve $\Gamma(t)$ is a straight segment aligned with $\boldsymbol{e}_x$.

2 Flow conditions

The flag interacting with a flow is probably the simplest setup one may imagine where a fluid flow and a thin structure interact. Let us consider its implementation as shown in figure 1 : in a two-dimensional channel with no-slip at the wall, a fluid flow is generated through incoming flow boundary condition with a constant profile. By volume conservation, the same is imposed as an outflow condition. In the middle of the channel is a thin, inextensible structure fixed at its windward end $\boldsymbol{A}$, while the leeward end $\boldsymbol{B}$ is free to move. In order to avoid a pointwise boundary condition at $\boldsymbol{A}$, which is mathematically and physically impractical, $\boldsymbol{A}$ is connected to a short plate acting as a pole, which is aligned with the flow.

This two-dimensional setup is very reminiscent (except for the geometry of the pole) of the experiment of a thread interacting with a film of soap found in [7]. If the thread is initially aligned with the flow, and no destabilistion occurs, this system mimics the Prandtl problem of the flow past an infinitely wide plate, in this case, with a finite length of the plate. However, as shown by [7] and commonly experienced with flags in the wind, this setup is subject to an instability that can be described as flapping.

Tension is the analogue of incompressible fluid's pressure within an inextensible structure. It acts so as to maintain the structure length constant, locally. At $\boldsymbol{B}$ in our setup, tension is zero because there is no other force acting pointwise to oppose it. At $\boldsymbol{A}$, the whole of the drag force exerted on the flag by the fluid has to be balanced by the pole, which thus feels a force equal to the tension of the flag at this point.

A thin structure, inextensible in its tangent plane, may still exhibit elasticity with respect to bending. In the limit of infinitely thin structures, this is described by the Helfrich bending energy [8], which is proportional to the square of the curvature of the structure.

3 Modelling and numerical technique

We assume that there is no slip on the flag, thus the velocity $\boldsymbol{u}$ of the fluid and flag are equal on $\Gamma(t)$. The total energy budget of the flag can then be monitored using:

$$\tilde{J}(\tilde{\boldsymbol{u}}) = \frac{d}{d\tilde{t}}\left(\frac{1}{2}\rho\int_\Omega \tilde{\boldsymbol{u}}^2 d\tilde{x} + \frac{1}{2}\lambda\int_{\Gamma(t)} \tilde{\boldsymbol{u}}^2 d\tilde{s} + \frac{1}{2}K_b\int_{\Gamma(t)} |\tilde{\kappa}|^2 d\tilde{s}\right) + \eta\int_\Omega |\tilde{\mathbb{D}}(\tilde{\boldsymbol{u}})|^2 d\tilde{x} \tag{1}$$

where ρ is the fluid surfacic density, λ the structure lineic density, K_b the bending modulus and η the fluid viscosity. $\kappa(\tilde{s})$ denotes the local curvature of the curve $\Gamma(\tilde{t})$, $\mathbb{D}(\boldsymbol{u})$ the rate of deformation tensor. The tilde denotes dimensional variables, their nondimensional counterparts is introduced in the sequel. The first two terms correspond to the variation of, respectively, fluid and structure kinetic energy, the third, the variation of bending energy and the last one the rate of viscous dissipation. Minimizing the total energy of the system is equivalent to minimizing its variation J. We provide boundary conditions at the exterior boundaries and around the flat plate at which the flag

is fixed:

$$\tilde{\boldsymbol{u}} = U\boldsymbol{e}_x \qquad \text{on } \Gamma_F, \qquad\qquad \tilde{\boldsymbol{u}} = \boldsymbol{0} \qquad \text{on } \Gamma_D;$$
$$\frac{\partial \tilde{u}_x}{\partial \tilde{y}} = 0,\ \tilde{u}_y = 0 \qquad \text{on } \Gamma_S. \tag{2}$$

and initial conditions $\Gamma(0) = \Gamma^0$, $\boldsymbol{u} = \boldsymbol{u}^0$. The fluid is considered incompressible and the structure inextensible, which can be written as,

$$\widetilde{\operatorname{div}}\,\tilde{\boldsymbol{u}} = 0 \qquad \text{in } \Omega, \qquad\qquad \widetilde{\operatorname{div}_s}\,\tilde{\boldsymbol{u}} = 0 \qquad \text{on } \Gamma(\tilde{t}). \tag{3}$$

Thus at any instant $\tilde{t}$ the problem writes as a constrained minimisation problem, finding $\tilde{\boldsymbol{u}}$ such that $\tilde{J}(\tilde{\boldsymbol{u}})$ is minimal subject to the boundary conditions (2) and the constraints (3).

We also need to describe the time evolution of the curve $\Gamma(\tilde{t})$ that represents the flag, $\Gamma(\tilde{t}) = \left\{\tilde{\gamma}(\tilde{t},\ \tilde{s}),\ \tilde{s} \in [0, L]\right\}$, and:

$$\tilde{\boldsymbol{\gamma}}(\tilde{t}, \tilde{s}) = \tilde{\boldsymbol{\gamma}}_0(\tilde{s}) + \int_0^{\tilde{t}} \tilde{\boldsymbol{u}}(\tilde{\tau},\ \tilde{\boldsymbol{\gamma}}(\tilde{\tau}, \tilde{s}))\,\mathrm{d}\tilde{\tau}, \tag{4}$$

Non dimensionalising using the length of the flag L and the incoming velocity U, we obtain the groups $\mathrm{Re} = \rho UL/\eta$, Reynolds number of the fluid, $\mathrm{Re}_\Gamma = \lambda U/\eta$, Reynolds number of the flag, and $C_\kappa = \eta LU^2/K_b$ which is associated with bending rigidity. Before we can characterise the minimum of the functional J, the bending rigidity term needs to be explicited. Using the identity $\boldsymbol{a}^2\boldsymbol{b}^2 = (\boldsymbol{a}\cdot\boldsymbol{b})^2 + (\boldsymbol{a}\times\boldsymbol{b})^2$, the curvature can be written as $\kappa = \left(\boldsymbol{\gamma}_{,ss}^2\boldsymbol{\gamma}_{,s}^2 - (\boldsymbol{\gamma}_{,ss}\cdot\boldsymbol{\gamma}_{,s})^2\right)/|\boldsymbol{\gamma}_{,s}|^6$ (using the compact derivation notation $a_{,s} = \partial a/\partial s$). We obtain [9] that,

$$\frac{\mathrm{d}}{\mathrm{d}t}\int_{\Gamma(t)} \kappa^2\,\mathrm{d}s = \left[\kappa u_{n,s} + \kappa^2 u_t\right]_A^B + \int_{\Gamma(t)} \left(\kappa_{,s}\boldsymbol{u}_{,s}\cdot\boldsymbol{n} + \kappa^3\boldsymbol{u}\cdot\boldsymbol{n} + \kappa\kappa_{,s}\boldsymbol{u}\cdot\boldsymbol{t}\right)\,\mathrm{d}s \tag{5}$$

$$= \left[\kappa u_{n,s} + \kappa^2 u_t\right]_A^B + \int_{\Gamma(t)} \left(\kappa_{,ss} + \frac{\kappa^3}{2} + \frac{\kappa_{,s}}{2}\delta_{\{\boldsymbol{A},\boldsymbol{B}\}}\right)\boldsymbol{u}\cdot\boldsymbol{n}\,\mathrm{d}s \tag{6}$$

where u_n and u_t are normal and tangential components of $\boldsymbol{u}$. Equation (6) is obtained by applying Green's formula to (5). Both equations present boundary terms. The first two boundary terms are common to both formulations, corresponding to the shear force at these points. The last term, appearing explicitly only in equation (6) (where we have written it as a Dirac mass within the integral), corresponds to the bending moment. Thus additional boundary conditions need to be imposed in order to fully describe the problem. At point $\boldsymbol{A}$, the velocity is already fixed to zero, so that only the shear force boundary condition needs to be imposed. Since there is no pointwise shear source, we set $\kappa(\boldsymbol{A}) = 0$. At the free end point $\boldsymbol{B}(t)$, there is no pointwise force at all, so both shear force and bending moment need to be imposed. We get,

$$\kappa(\boldsymbol{A}) = 0 \qquad\qquad \kappa(\boldsymbol{B}) = 0 \qquad\qquad \frac{\partial\kappa}{\partial s}(\boldsymbol{B}) = 0 \tag{7}$$

We can now characterise a saddle point of the Lagrange functional associated with equation (1) and (3), see [6], using equation (5) which allows to impose only in a weak sense the third boundary condition in equation (7). The problem is thus to find $\boldsymbol{u}$, p and ζ, respectively the velocity, pressure and tension in the flag, in spaces $V \times L_0^2(\Omega) \times Z(t)$ defined as:

$$V = \left\{\boldsymbol{v} \in H^1(\Omega),\ \boldsymbol{v} = 0 \text{ on } \Gamma_D,\ \boldsymbol{v} = U\boldsymbol{e}_x \text{ on } \Gamma_F\right\},$$
$$Z(t) = \left\{\zeta \in H^{1/2}(\Gamma(t)),\ \exists\theta \in H_{00}^{1/2}(\Gamma(t)\cup\Gamma_D),\ \zeta = \theta_{|_{\Gamma(t)}}\right\},$$

such that:

$$\mathrm{Re}\,\frac{\mathrm{d}}{\mathrm{d}t}\int_{\Gamma(t)} \boldsymbol{u}\cdot\boldsymbol{v}\,\mathrm{d}s + \mathrm{Re}_\Gamma\frac{\mathrm{d}}{\mathrm{d}t}\int_{\Gamma(t)} \boldsymbol{u}\cdot\boldsymbol{v}\,\mathrm{d}s + \int_\Omega 2\mathbb{D}(\boldsymbol{u}) : \mathbb{D}(\boldsymbol{v})\,\mathrm{d}x$$
$$+\frac{1}{2C_\kappa}\int_{\Gamma(t)} \left(\kappa\kappa_{,s}\boldsymbol{v}\cdot\boldsymbol{t} + \kappa^3\boldsymbol{v}\cdot\boldsymbol{n}\right) - (\kappa_{,s}\boldsymbol{v}_{,s})\cdot\boldsymbol{n}\,\mathrm{d}s$$
$$-\int_\Omega p\operatorname{div}\boldsymbol{v}\,\mathrm{d}x - \int_{\Gamma(t)} \zeta\operatorname{div}_s\boldsymbol{v}\,\mathrm{d}s = 0 \qquad \forall\boldsymbol{v} \in H_0^1(\Omega) \tag{8}$$
$$-\int_\Omega q\operatorname{div}\boldsymbol{u}\,\mathrm{d}x = 0 \qquad \forall q \in L^2(\Omega), \tag{9}$$
$$-\int_{\Gamma(t)} \xi\operatorname{div}_s\boldsymbol{u}\,\mathrm{d}s = 0 \qquad \forall\xi \in Z(t). \tag{10}$$

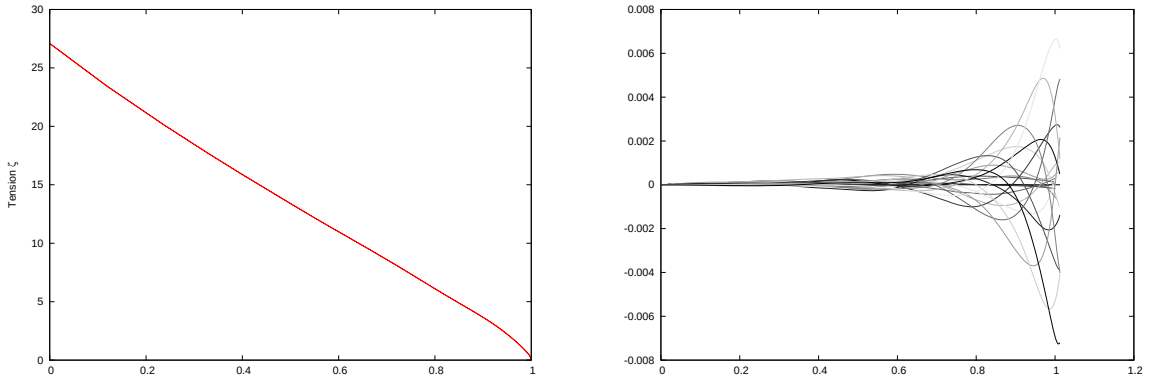

(a) (b)

Figure 2: Flow past a flag problem for $\mathrm{Re} = 1000$, $\mathrm{Re}_\Gamma = 25$ and $1/\mathrm{C}_\kappa = 0$. (a) Tension in the flag when maintained straight in the flow (initial condition). (b) Time evolution of the flag configuration. Gray level codes time evolution, from dark to light, $t = 0$ to $t = 5120$, dark to light again, $t = 5632$ to $t = 10240$.

In order to approximate this problem with finite elements, we introduce the piecewise linear curve Γ_h^0 whose segments are advected with the velocity at their endpoints to obtain Γ_h^{n+1} from Γ_h^n. A triangulation $\mathcal{T}_h^n$ whose edges include Γ_h^n is defined either by mesh generation (for $n = 64k$ with k an integer) or by advection of $\mathcal{T}_h^{n-1}$ with the velocity at its nodes. The following finite element spaces [6] are employed:

$$V_h^n = V \cap P_2(\mathcal{T}_h^n) \cap C^0(\Omega), \quad Q_h^n = P_2(\mathcal{T}_h^n) \cap C^0(\Omega \setminus \Gamma_h^n), \quad Z_h^n = \{\xi_h \in P_2(\Gamma_h^n),\, \xi_h(\boldsymbol{B}) = 0\} \cap C^0(\Gamma_h^n).$$

The resolution within these spaces of equations (8, 9, 10) yields a linear system in the nodal values $(U,\, P,\, Z)$ of $(\boldsymbol{u}_h,\, p_h,\, \zeta_h)$ which has the form:

$$\begin{pmatrix} A & B^T & C^T \\ B & 0 & 0 \\ C & 0 & 0 \end{pmatrix} \begin{pmatrix} U \\ P \\ Z \end{pmatrix} = \begin{pmatrix} 0 \\ 0 \\ 0 \end{pmatrix}$$

which can be solved using Uzawa algorithm [10].

4 Numerical simulations

We perform numerical simulations using $\Omega = (-5,\, 25) \times (-3,\, 3)$, $\Gamma_D = (-0.5,\, 0) \times 0$. We take γ_0 equal to $(s,\, 0)$ for $s \in (0, 1)$ and compute the permanent flow first for a fixed flag (homogeneous Dirichlet boundary condition on the flag) at a given Reynolds number for the fluid, and set this solution as the initial condition of the calculation with the fluid-structure interactions.

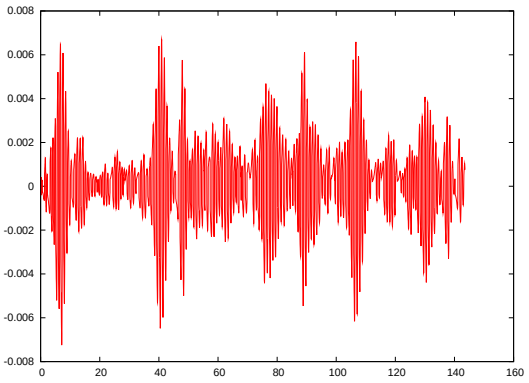

Figure 3: y-position of the endpoint of the flag as a function of time for $\mathrm{Re} = 1000$, $\mathrm{Re}_\Gamma = 20$ and $1/\mathrm{C}_\kappa = 0$.

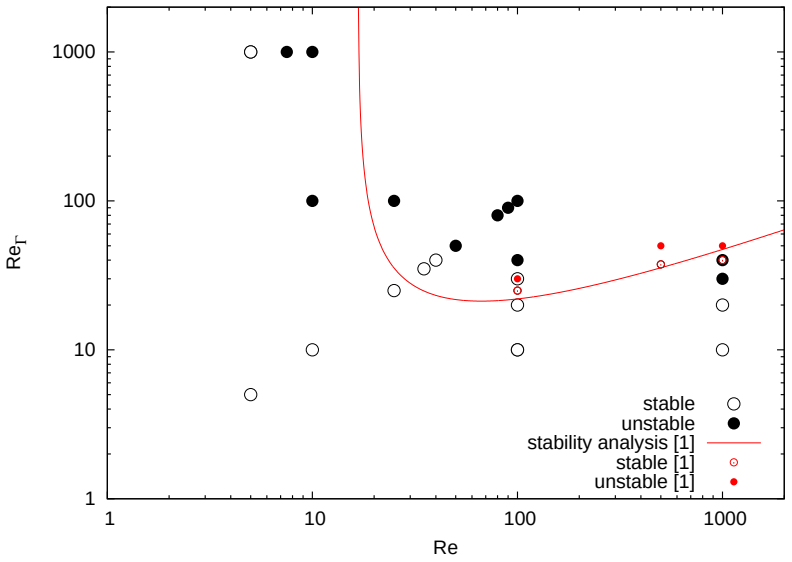

Figure 4: Stability diagram of the flow past a flag problem for $1/\mathrm{C}_\kappa = 0$. Red points, numerical results of [1]. Red line, linear stability analysis of [1], assuming that the tension is constant, $\zeta^C = 1.3\sqrt{\mathrm{Re}}$.

When either the fluid or the flag has no inertia, the only stable solution is having the flag aligned with the flow. This situation mimicks the flow past a finite plate, and is studied in [6]. Above a certain threshold for both Reynolds numbers, numerical noise (in our unstructured mesh approach) is sufficient to trigger flag destabilisation. Figure 2 summarises the time evolution of this destabilisation for $\mathrm{Re} = 1000$ and $\mathrm{Re}_\Gamma = 25$. It is seen that only part of the flag, on the lee-side, experiences flapping motion, the wind-part of the flag being kept aligned with the incoming flow. This can be understood because tension is lower on the lee-side, while the destabilising effect of the difference of momentum of the flag and flow is unchanged, as will be seen in the next section. The amplitude of flapping increases in a near-exponential manner up to a maximum of 0.05 in this case.

For a slightly lower Reynolds number of the structure, $\mathrm{Re}_\Gamma = 20$, the amplitude of flapping decreases after an initial transient increase. However, small pertubations originating from numerical simulation noise are able to destabilise again the flag, leading to a succession of flapping bursts and damping, see figure 3.

In figure 4 we plot the stability diagram of the system, using a small polynomial perturbation of class C^3 of amplitude 10^{-4} for $0 < s < 0.1$ superimposed to the aligned configuration for the flag, in order to speed up destabilisation. Although destabilisation is observed for similar values of the Reynolds numbers as in a previous linear stability analysis by Connell and Yue [1], the agreement is far from perfect. Stability analysis in this paper is recalled here. An evolution equation for the flag, using the slender body approximation to account for the hydrodynamic forces that the fluid exerts on the flag, is written as:

$$\mathrm{Re}_\Gamma \frac{\partial^2 y}{\partial t^2} - \mathrm{Re}\frac{\partial}{\partial x}\left(T\frac{\partial y}{\partial x}\right) + \frac{1}{\mathrm{C}_\kappa}\frac{\partial^4 y}{\partial x^4} + a\mathrm{Re}\left(\frac{\mathrm{D}}{\mathrm{D}t}\right)^2 y = 0 \tag{11}$$

where a is the added mass coefficient. In [11], the author obtains from potential flow calculation that $a = 2\pi/k$, where k is the wavelength of the disturbance, this is the assumption made in [1]. This differs from the more detailed analysis of added mass effect in [2]. Connell and Yue also assume a uniform tension T in the flag, which as they state is a gross approximation of the decreasing tension, see numerical result in figure 2(a).

5 Discussion

We present and demonstrate the capability of a novel, monolithic numerical method for solving fluid–thin structure interaction problems, with an inextensible structure. This is an extension of the method presented in [6] to structures having an inertia and a bending elasticity. In this method, the forces associated with the structure are treated as Robin-type boundary conditions.

Numerical calculations are then presented for a classical fluid-structure problem, the flow past a flag. The calculations we present are the first in this parameter range, which present a difficulty for the stability of the structure, leading previous authors to use stabilising terms when approaching this parameter range.

References

1. B. S. H. Connell and D. K. P. Yue. Flapping dynamics of a flag in a uniform stream. *J. Fluid Mech.*, 581:33–67, 2007.
2. M. Argentina and L. Mahadevan. Fluid-flow-induced flutter of a flag. *Proc. Natl. Acad. Sci. USA*, 102:1829–1834, 2005.
3. A. Manela and M. S. Howe. The forced motion of a flag. *J. Fluid Mech.*, 635:439–454, 2009.
4. C.S. Peskin. The immersed boundary method. *Acta Numerica*, 11:479–517, 2002.
5. P. B. Ryzhakov, R. Rossi, S. R. Idelsohn, and E. Oñate. A monolithic lagrangian approach for fluid–structure interaction problems. *Comput. Mech.*, 46:883–889, 2010.
6. J. Étienne, J. Lohéac, and P. Saramito. Inextensible membranes or threads immersed in a fluid: a lagrange multiplier approach. In *Congrès Français de Mécanique*, Besançon, France, September 2011 (under review).
7. J. Zhang, S. Childress, A. Libchaber, and M. Shelley. Flexible filaments in a flowing soap film as a model for one-dimensional flags in a two-dimensional wind. *Nature*, 408:835–838, 2000.
8. W. Helfrich. Elastic properties of lipid bilayers: Theory and possible experiments. *Z. Naturforsch.*, 28C:693–793, 1973.
9. B. Balde. Interactions fluide–structure mince : drapeau flottant au vent. Master's thesis, École nationale supérieure d'ingénieurs du Sud Alsace et Université de Haute-Alsace à Mulhouse, Laboratoire de Spectrométrie Physique, UMR 5588 CNRS–UJF, Grenoble, 2010.
10. M. Fortin and R. Glowinski. *Augmented Lagrangian methods, applications to the numerical solution of boundary value problems*. Elsevier Science, Amsterdam, 1983.
11. R. Coene. Flutter of slender bodies under axial stress. *Appl. Sci. Res.*, 49:175–187, 1992.